

We are IntechOpen, the world's leading publisher of Open Access books Built by scientists, for scientists

6,900

Open access books available

186,000

International authors and editors

200M

Downloads

Our authors are among the

154

Countries delivered to

TOP 1%

most cited scientists

12.2%

Contributors from top 500 universities



WEB OF SCIENCE™

Selection of our books indexed in the Book Citation Index
in Web of Science™ Core Collection (BKCI)

Interested in publishing with us?
Contact book.department@intechopen.com

Numbers displayed above are based on latest data collected.
For more information visit www.intechopen.com



Molecular Signature in Human and Animal Prion Disorders

Michele Fiorini, Matilde Bongianni and
Gianluigi Zanusso

Additional information is available at the end of the chapter

<http://dx.doi.org/10.5772/67329>

Abstract

In human and animal transmissible spongiform encephalopathies (TSEs) or prion disorders, biochemical analysis of disease-associated prion protein (PrP^{TSE}) is a first-line approach for large scale routine testing and for a rapid molecular typing. This characterization is based on conformational properties of PrP^{TSE} enciphered in its secondary and tertiary structures and on glycosylation profile. Several biochemical approaches are helpful in distinguishing PrP^{TSE} forms in human prion diseases. In particular, in sporadic Creutzfeldt-Jakob disease (CJD), PrP^{TSE} is characterized by two main glycotypes conventionally named PrP^{TSE} type 1 and PrP^{TSE} type 2 based on the apparent gel migration at 19 kDa and 17.5 kDa and glycoform ratio. Further, there are PrP^{TSE} low molecular weight fragments which correlate to distinct phenotypes of sCJD. Finally, by using two-dimensional PAGE analysis, which separates PrP^{TSE} on both isoelectric point and molecular size, we were able to detect two distinct migration pattern in PrP^{TSE} type 2, one in subjects with MM at codon 129 and another in MV, VV. We here provide an extensive PrP^{TSE} biochemical analysis in humans and animals affected with prion disorders. Further, we showed that PrP^{TSE} glycotypes observed in CJD shared similarities with PrP^{TSE} in bovine spongiform encephalopathies (BSEs). These signature similarities obtained by a biochemical analysis had been further confirmed by experimental transmission.

Keywords: prion protein, pathological prion protein, transmissible spongiform encephalopathies, prion disorders, protease-resistant PrP, biochemical phenotype, conformational assays, two-dimensional analysis, amyloid

1. Introduction

Prion diseases, or transmissible spongiform encephalopathies (TSEs), are fatal neurodegenerative disorders affecting humans and animals with a sporadic, genetic, or iatrogenic etiology [1]. The crucial event in the pathogenesis of TSEs is the conformational conversion of the normal cellular prion protein (PrP^C) into a pathologic isoform (PrP^{TSE}), which is self-propagating and infectious [2]. PrP^C is a glycosylphosphatidylinositol (GPI) anchored protein residing on the outer leaflet of the cellular membrane of most cell types in mammals. It is synthesized as 253 amino acids polypeptide before being posttranscriptionally modified by the cleavages of 22 amino acids of signal sequence at N-terminal and of 23 amino acids at the C-terminal for adding GPI anchor. The mature protein contains a disulfide bond between Cys179 and Cys214 and can be glycosylated at Asn181 and Asn197. While PrP N-terminus contains a variable number of octapeptide repeats, it is flexible and disordered, and C-terminus is more structured in a globular domain characterized by three α -helices and two short β -sheet structures [3]. Structurally, PrP^C contains mainly α -helix structures, while PrP^{TSE} contains β -sheet structures [4]. These conformational changes in secondary and tertiary structures determine PrP^{TSE} specific physicochemical changes such as PK resistance, insolubility in nonionic detergents and high propensity to aggregate in oligomers of different size [5]. It has been assessed that PrP^{TSE} conformations are related to distinct prion strains, which propagate with specific transmission properties in susceptible mammals (different infectious properties, incubation times or neuropathological lesions) [6]. Aim of the present chapter is to describe different biochemical strategies to characterize molecular features and biochemical properties of prions in humans and animals.

1.1. Defining molecular features of prions by biochemical analysis, cellular and disease-associated PrP biochemical characterization

A suitable way to detect and reveal PrP^C and PrP^{TSE} is Western Blot analysis following electrophoretic mono-dimensional (1D) separation [7]. Electrophoretic analysis provides information about glycoform based on PrP molecular weight and glycosylation profile [8]. Two-dimensional (2D) electrophoretic analysis is a more in depth analysis to investigate the molecular features of proteins, improving the resolution since a single amino acid substitution in PrP sequence, glycosylation profile or the presence or absence of GPI anchor is sufficient for determining a shift pointing migration. The goal of 2D electrophoresis is to characterize PrP^{TSE} molecular signature typical of each prion strain, more accurate and specific than simple classical 1D electrophoretic pattern.

1.2. Conformational assays to characterize PrP^{TSE} biochemical properties in human and animal prion disorders

Several simple biochemical methods can be used to investigate conformational features of different biochemical prion strains.

1.2.1. Resistance to proteinase K treatment

Western blot analysis following PK digestion allows the detection of PK-resistant PrP, also termed PrP²⁷⁻³⁰. This method is routinely used to confirm TSEs diagnosis.

Biochemical strains of PrP^{TSE} can be defined also by the presence of PK resistant additional minor C-terminally truncated fragments (CTFs).

1.2.2. Detergent insolubility and separation by size of PrP^{TSE} aggregates

The high representation of β -sheet structures is a requisite of PrP^{TSE} to form insoluble aggregates in nonionic detergents. By ultracentrifugation, enriched fractions of PrP^{TSE} can be prepared and separated by different size of aggregates in sucrose gradients. This analysis allows to characterize PrP^{TSE} conformational properties in a given prion strains.

1.2.3. Conformational stability in increasing concentration of GdnHCl

Different prion strains show different conformational stability, which can be assessed by PK-resistance testing following exposure to different denaturing or nondenaturing conditions.

2. PrP conformers and disease phenotypes in human and animal TSEs

2.1. 1D analysis of molecular strains

2.1.1. Human prion disorders

2.1.1.1. Sporadic forms

In human prion disorders, several different PrP^{TSE} types have been described, based on the electrophoretic migration and the glycosylation profile of PrP²⁷⁻³⁰. This is composed of a major triplet of bands, which represent the differently glycosylated isoforms of PrP^{TSE}. Since prions are associated with distinct conformations, biochemical analyzes are useful to define prion strains.

In human sporadic CJD, PrP^{TSE} separates as two main glycotypes: PrP^{TSE} type 1 and PrP^{TSE} type 2A with an apparent gel migration of the unglycosylated isoform at 21 kDa and 19 kDa respectively (**Figure 1A**) [9]. Type-1 and 2A show similar glycosylation profile (**Figure 1B**).

In 2007, we reported on a novel PrP^{TSE} glycoform, showing a predominant unglycosylated isoform and slightly the monoglycosylated isoform, but completely lacking the diglycosylated one, named Type-U (**Figure 1A and B**) [10].

In 2010, an additional form of prion disease has been described, called variably protease-sensitive prionopathy (VPSPr). VPSPr is characterized not only by a distinct disease phenotype but also by a ladder-like electrophoretic profile of the PK-resistant PrP^{TSE} fragments (**Figure 1C**). The ladder-like profile consisted of five major bands migrating at approximately 26 kDa, 23 kDa, 20 kDa, 17 kDa, and 7 kDa [11].

2.1.1.2. Genetic forms

Familial prion diseases, FFI and GSS are characterized by distinct biochemical profiles, with typical migration properties, glycosylation profiles or truncated fragments expression. While fCJD

and FFI show the presence of PrP²⁷⁻³⁰ differentially PK cleaved and glycosylated, in GSS PrP²⁷⁻³⁰ is absent, pathological PrP is composed of internal fragments of 8 and 11 kDa with the exception of P102L. P102L shows a peculiar pattern with the presence of both PrP²⁷⁻³⁰ and 8 kDa internal fragment. Familial prion diseases western blot is schematically reported in **Figure 1C** [12–14].

2.1.1.3. Infectious form

Following BSE transmission to humans causing variant CJD (vCJD), a new human molecular strain was defined (type 2B) with a molecular weight comparable to type 2A but with a prevalent diglycosylated isoform (**Figure 1C**) [15].

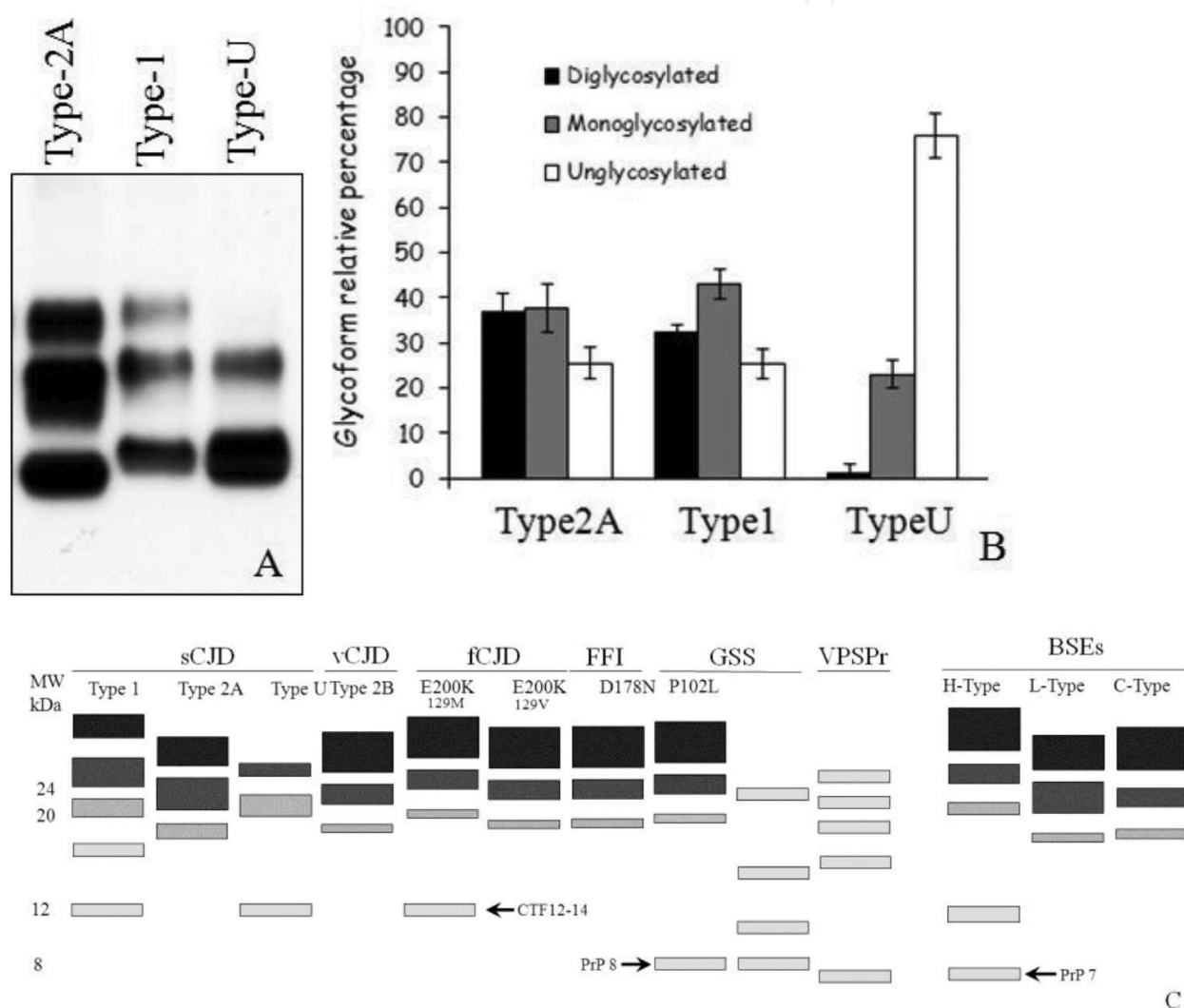


Figure 1. (A) Western blot profile of three sCJD molecular strains and their relative glycoform profile (B). (C) Schematic representation of human western blot profile of sporadic, genetic and acquired CJD molecular types.

2.1.2. Size aggregates

Since the abundance of β -sheet in the secondary structure of PrP^{TSE} confers the tendency to aggregate, ultracentrifugation procedures can be applied to discriminate different con-

formational states associated with different prion strains. By using ultracentrifugation in sucrose gradients and sarkosyl, insolubility and the size of PrP^{TSE} aggregates can be compared [16].

The three sporadic molecular subtypes are characterized by distinct sedimentation patterns, considering ultracentrifugation analysis before and after PK treatment (**Figure 2**). MV-1 PrP species are distributed at the beginning and at the end of the gradient, indicating the presence of small soluble forms and big insoluble aggregates; this distribution is maintained also after PK treatment. MV-2 sedimentation pattern of cellular PrP is characterized by a wide distribution all over the gradient, while after PK digestion PrP^{TSE} is detected as big insoluble aggregates at the end of the gradient. MV-U sedimentation pattern of cellular PrP is comparable to MV-1, but PrP^{TSE} species are found mainly at the bottom of the gradient as for MV-2.

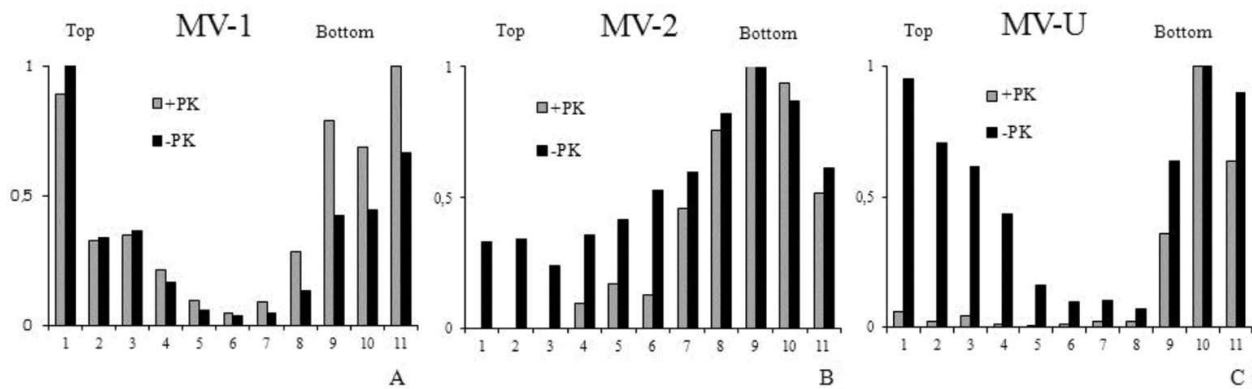


Figure 2. Fractionation of sCJD PrP aggregates. Brain homogenates from frontal cortices of MV-1 and MV-2 and MV-U were sedimented in a 10–60% sucrose gradient. After sedimentation, half samples were digested with PK. Relative cellular (black) and PK resistant (gray) percentage of fraction distribution in MV-1 (A), MV-2 (B) and MV-U (C).

2.1.3. Conformational stability assay

Sporadic human strains can be distinguished also by testing the strength of three dimensional protein structure against denaturing conditions. This is investigated by PK treatment after exposure to increasing amounts of guanidine [17].

In **Figure 3**, it can be noted that in MV-1 and MV-2, the structure integrity is maintained until an exposition to 2 M guanidine before PK can completely digest the protein; in MV-U, a concentration of 1.5 M is enough to unfold the PrP^{TSE}. It's interesting to note that in MV-U at a 1.0 M guanidine concentration, PK digestion produces two conformers of PrP^{TSE} at different molecular weights, indicating that two molecular strains are hidden in the three dimensional conformation (unpublished data). Inoculation experiments in bank voles have shown this MV-U case contains two different strains with different incubation time and different lesion profile associated with two different molecular electrophoretic patterns after transmission (unpublished data).

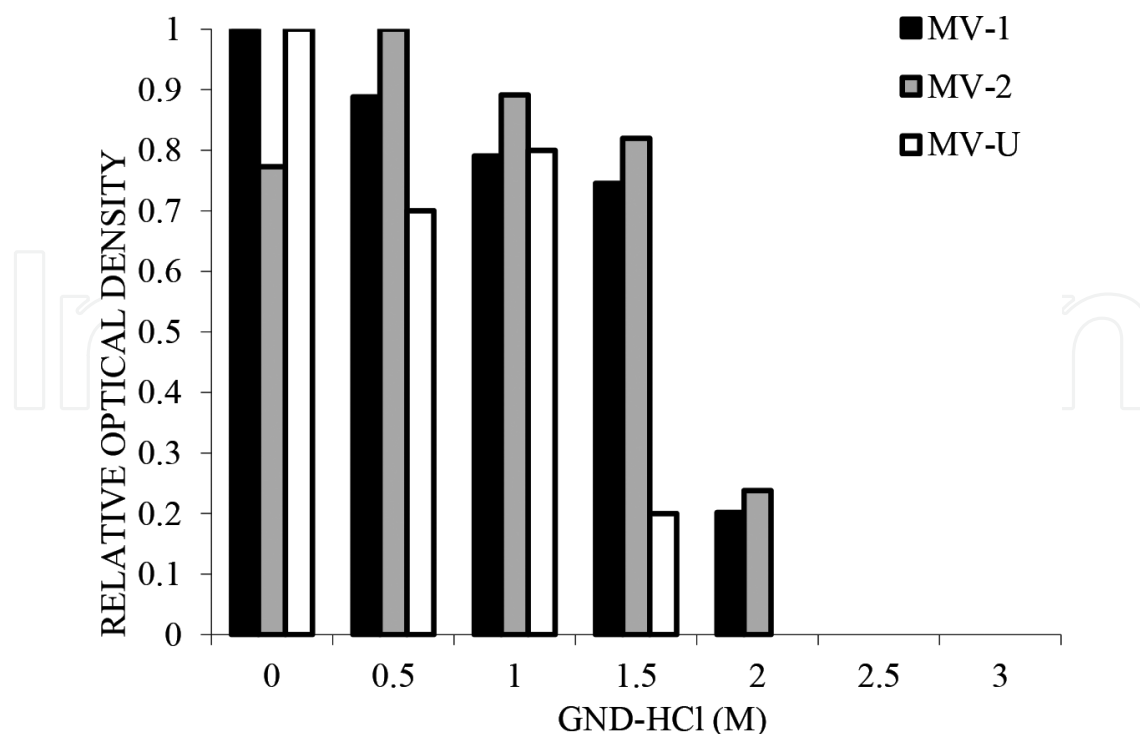


Figure 3. Relative quantification of denaturation transitions for MV-1, MV-2 and MV-U types.

2.2. 2D analysis of molecular strains

2.2.1. Molecular signature

2D analysis of PK and PNGase treated samples gives trains of spots corresponding to the nude N-ragged ended isoforms of the prion core fragment. Western blot using antibodies against the C-terminal of prions evidences also the presence of truncated fragments (CTFs) [18].

Two-dimensional immunoblot with anti-PrP antibodies gives the possibility to identify two groups of C-terminal protease-resistant PrP fragments. All sCJD cases with type 1 PrP²⁷⁻³⁰, in addition to MM subjects with type 2 PrP²⁷⁻³⁰, are characterized by the presence of CTFs of 16–17 kDa and 12–14 kDa. Conversely, brain homogenates from VV and MV patients with type 2 PrP²⁷⁻³⁰ contain CTFs migrating at 17.5–18 kDa. Therefore, we can conclude that the mechanism involved in the formation of CTFs is not influenced by codon 129 and by the type of PrP²⁷⁻³⁰.

Based on the biochemical patterns obtained by combining the PrP²⁷⁻³⁰ core fragment and lower truncated PrP species, three distinct groups or fingerprints of disease-associated PrP species in sCJD with type 1 PrP^{TSE}, MM2 subjects, and MV2/VV2 cases can be defined (**Figure 4**).

2.2.2. GPI anchor

PrP posttransductional modifications, such as the presence of GPI anchor can be easily investigated by 2D analysis [1]. 2D molecular coordinates (pI and Mw) of GPI anchor were calculated by comparing the unglycosylated PrP in wild type and anchorless transgenic mice. By 2D analysis, we can compare the 2D coordinates of known recombinant peptides with

unknown samples to see if their 2D coordinates correspond to the nude peptides of are shifted by the “weight” of the GPI anchor. Since recombinant protein molecular coordinates in 2D analysis correspond exactly to the theoretical values (**Figure 5**), anchored or anchorless prions can be identified by only valuating if the measured pI and Mw correspond to the theoretical ones with or without GPI weight.

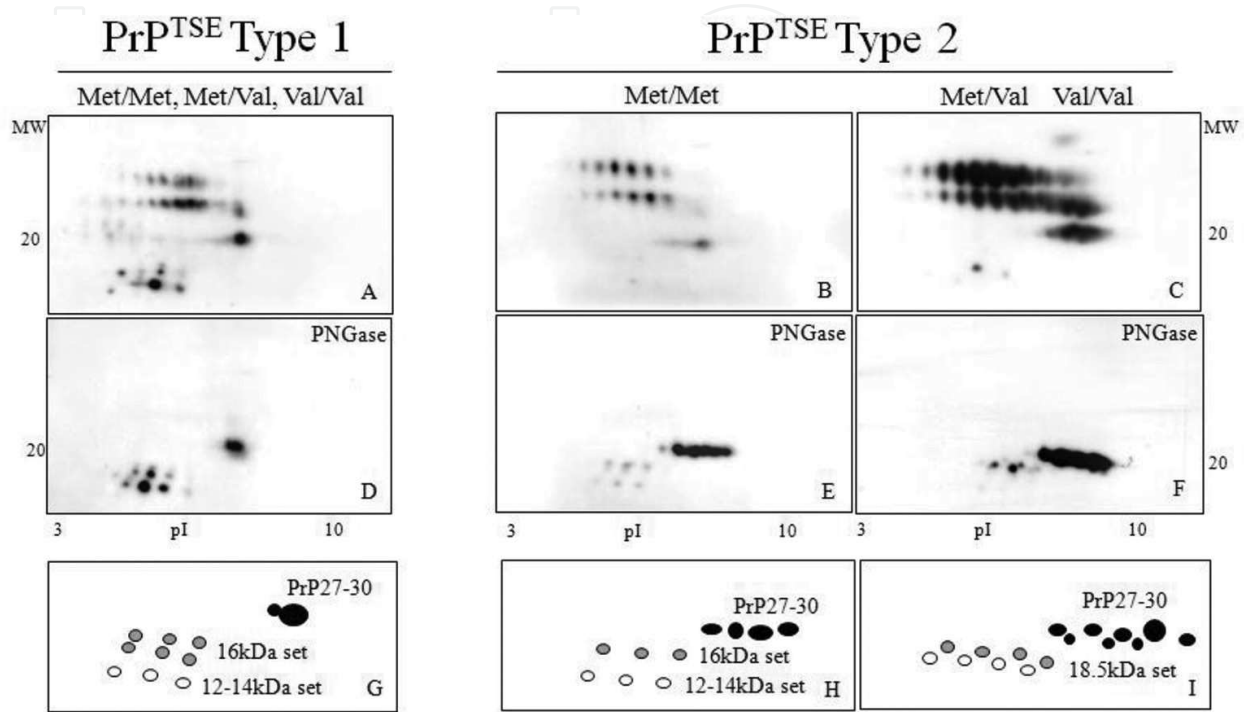


Figure 4. Two-dimensional mapping of sCJD brain homogenates after PK treatment (A–C) and deglycosylation (D–F) with anti-C-terminal antibody. Schematic diagram of PK-resistant C-terminal PrP core fragments in sCJD subtypes. (G, H, I) [17].

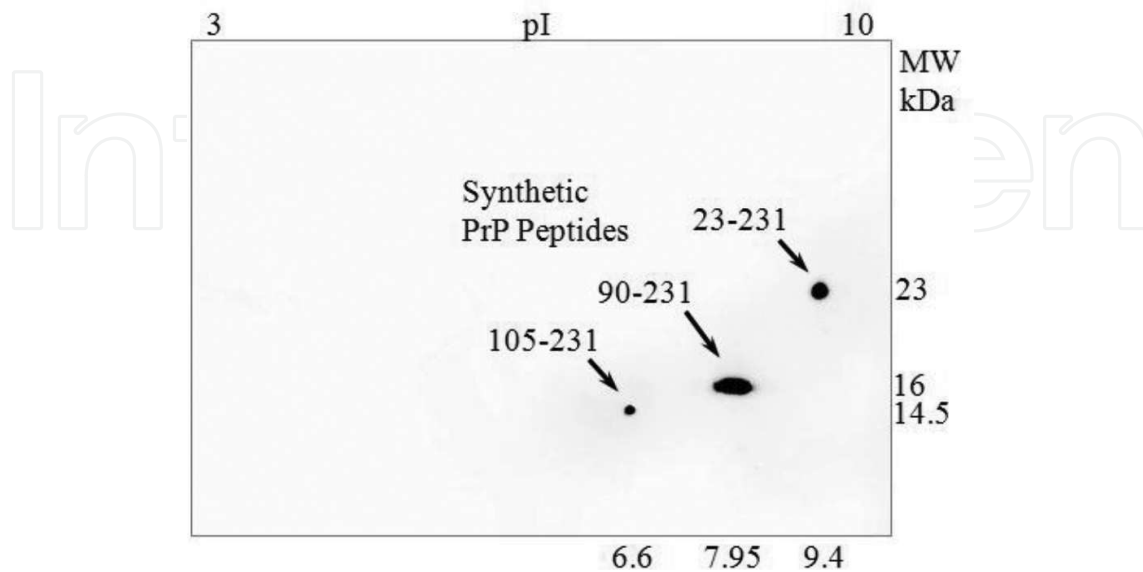


Figure 5. Two-dimensional mapping of synthetic PrP peptides [1].

Figure 6 represents a schematic picture of PrP^{TSE} core fragment after 2D analysis [1].

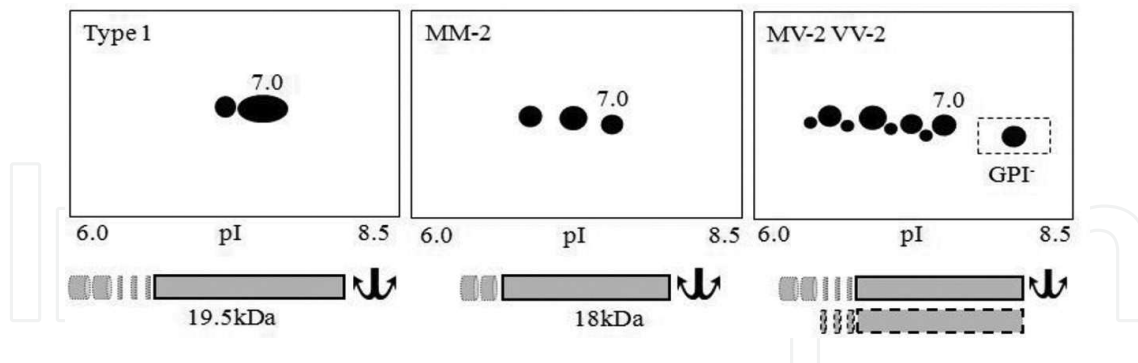


Figure 6. Schematic representation of anchored and anchorless PK-resistant PrP core fragments in sCJD subtypes.

All the sCJD molecular type 1 and 2 subtypes have all the 27–30 isoforms with a pI more acidic than pH 7 except the group MV-2/VV-2 showing an extra isoform at pI ~ 8. This last isoform has the same molecular coordinates of the synthetic peptide 90–231 and corresponds to anchorless form. All other spots identify anchored PrP^{TSE} forms, since their pI is shifted about 1 pH unit toward the acidic pole.

2.3. Cattle

2.3.1. Animal prion disorders

Since it was known, BSE was always described by the same molecular strain characterized by a diglycosylated electrophoretic pattern. In 2004, in Italy, two old cows were described by Zanusso et al. as showing a lower molecular weight of the prion core fragment and a different glycosylation pattern at western blot [19]. In 2007, other cases were found in France with classical glycosylation profile but with higher molecular weight of the prion electrophoretic profile (Figure 7) [20]. These new atypical molecular types were named BASE (bovine amyloidotic spongiform encephalopathy) or L-type BSE and H-type BSE considering the lower or higher western blot profile. The three molecular profiles also reflect different clinicopathological features of the diseases [21].

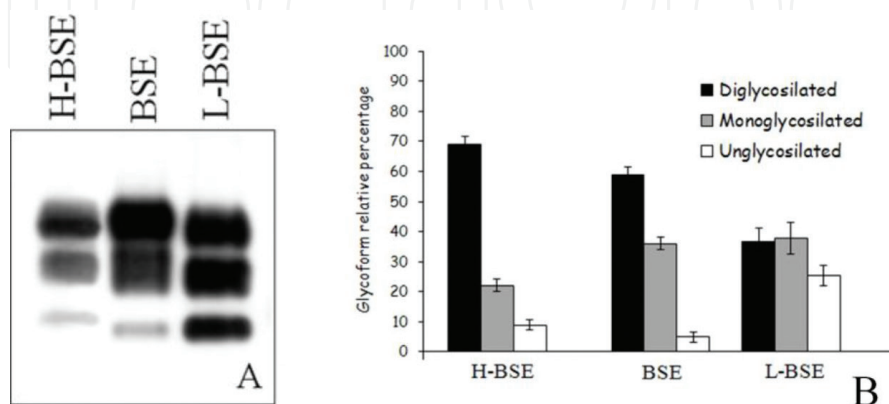


Figure 7. (A) Western blot profile of three BSE molecular strains and their relative glycoform profile (B).

2.3.1.1. Size aggregates

Ultracentrifugation analysis before PK treatment shows a similar sedimentation pattern in the three cattle molecular subtypes: samples present both small soluble forms and large insoluble aggregates. The treatment with PK shows PrP^{TSE} is present in the insoluble aggregates in all BSE strains (**Figure 8**); moreover, aclassical BSE shows also an additional small amount of soluble forms (**Figure 8C**).

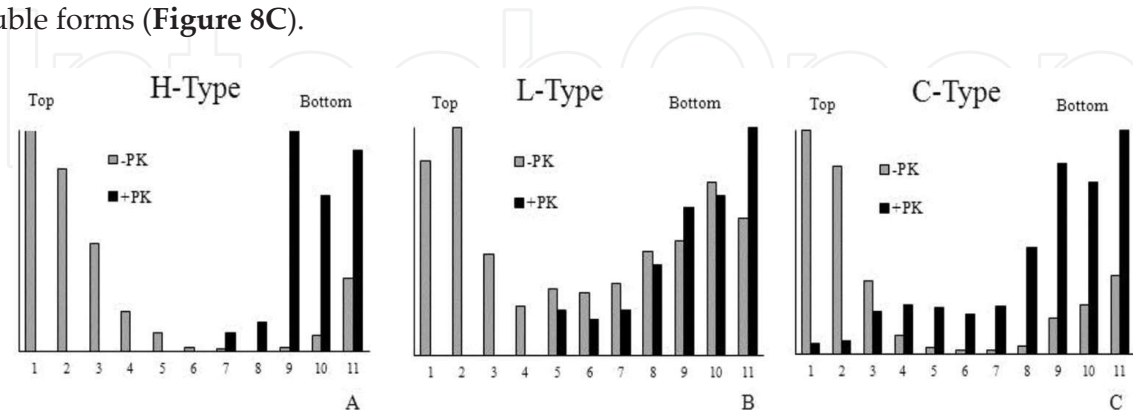


Figure 8. Fractionation of BSE PrP aggregates. Brain homogenates from frontal cortices of H-BSE and L-BSE and C-BSE were sedimented in a 10–60% sucrose gradient. After sedimentation, half samples were digested with PK. Relative cellular (gray) and PK resistant (black) percentage of fraction distribution in H-BSE (A), L-BSE (B) and C-BSE (C).

2.3.1.2. Conformational stability assay

Both atypical forms of BSE can be distinguished from classical BSE and also human sCJD on the basis of structure denaturation by chaotropic agents such as guanidine. While human sporadic PrP^{TSE} is digested after an exposition over 2 M guanidine, all BSE forms maintain a minimal Pk resistance until 3 M guanidine. Among BSEs, C-type is shown to be strongly resistant to Pk digestion until 2 M guanidine, while H- and L-type resistances are stable until 2.5 M (**Figure 9**).

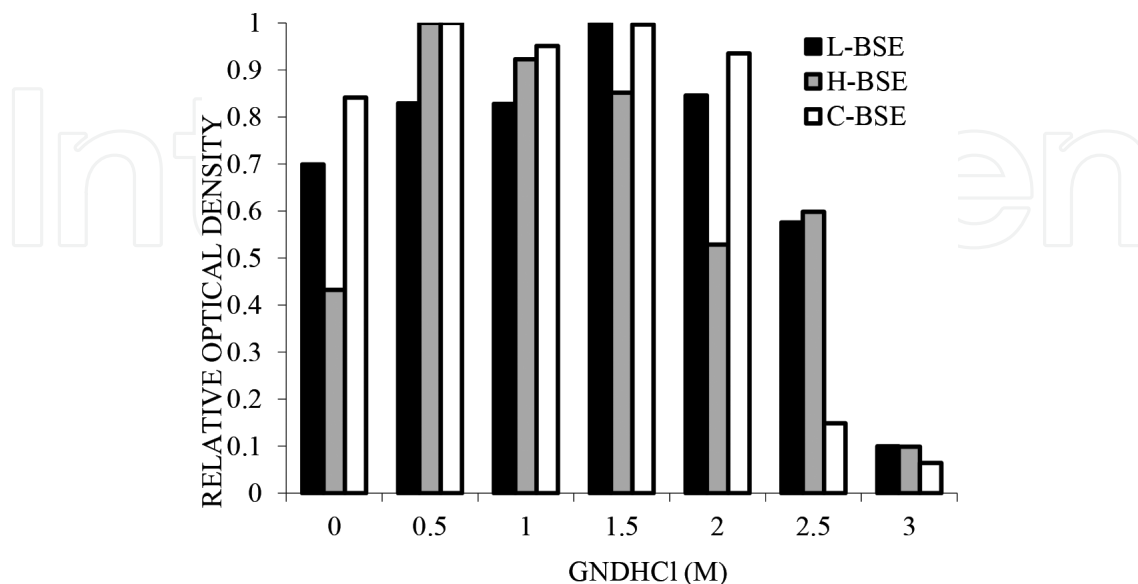


Figure 9. Relative quantification of denaturation transitions for the H-BSE, C-BSE, and L-BSE.

2.3.1.3. Molecular signature

In **Figure 10**, 2D analysis of typical and atypical BSE shows that the three forms of BSE correlate to three distinct signatures. H-type BSE shows a consistent representation of truncated fragments at 12 kDa, while C-type and L-type molecular fingerprint is mainly characterized by 27–30 PrP.

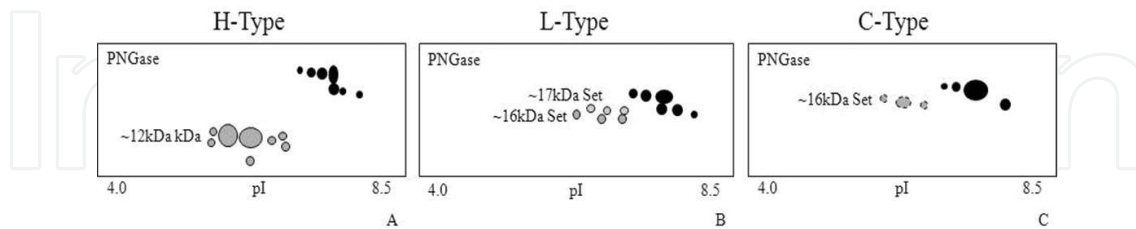


Figure 10. Two-dimensional mapping of BSE brain homogenates after PK treatment. Schematic diagram of PK-resistant C-terminal PrP core fragments in BSE strains (A–C).

2.3.1.4. GPI anchor

In the three forms of BSE, PrP₂₇₋₃₀ core fragment is characterized by two sets of isoforms differing of ~ 1.0 unit of pI and ~ 2.0 kDa (**Figure 11**).

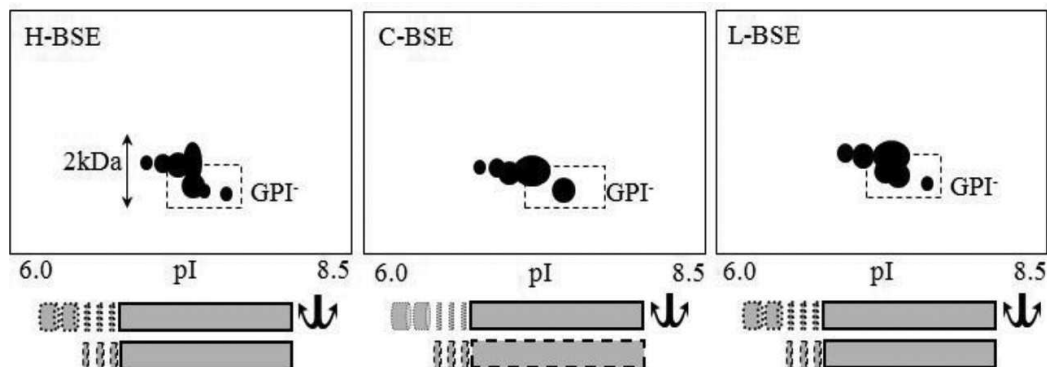


Figure 11. Schematic representation of anchored and anchorless PK-resistant PrP core fragments in BSE strains.

The comparison between theoretical and measured isoelectric points and molecular weights of core fragments indicates that the upper set represents anchored forms.

Therefore, classical BSE shows only one anchorless isoform, while in L-BSE and H-BSE, there are three anchorless isoforms with average amount comparable to the anchored ones.

2.4. Molecular similarities between human and cattle TSE forms

2.4.1. Comparison of human and cattle molecular strains by 1D analysis

In **Figure 12**, biochemical PrP^{TSE} types are matched two by two to best compare the molecular similarities. sCJD type 1 and H-type BSE share the same molecular weight; sCJD type 2A and L-type BSE show similar molecular weight and glycosylation profile; vCJD and classical BSE are characterized by a similar diglycosylated profile.

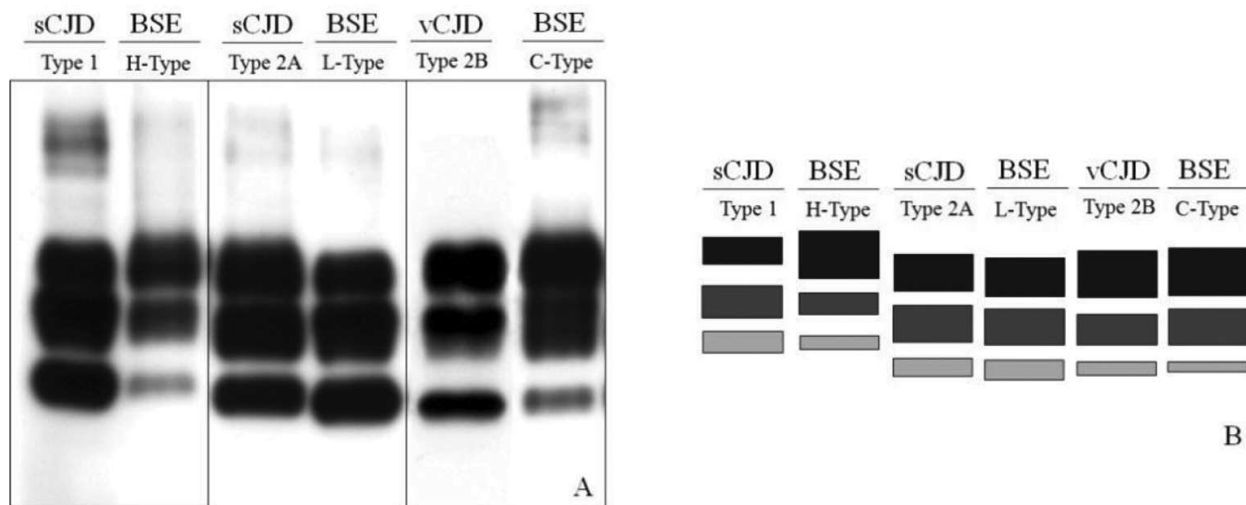


Figure 12. Western blot profile (A) and schematic representation of paired human and BSE strains (B).

2.4.2. Comparison of human and cattle molecular strains by 2D analysis

Increasing resolution power by 2D analysis, it's possible to deeply compare biochemical signatures of PrP^{TSE} between humans and cattle (**Figure 13**). PrP^{TSE} shows similar signatures in BSE-H and sCJD type 1 and is characterized by the dominance of C-terminal fragments. These patterns are distinct from those observed in other forms. Both sCJD type 2A and L-type BSE show the same set of spot at about 18 kDa, while in vCJD and L-BSE the molecular signature seems to be different.

2.4.3. Comparison of human and cattle molecular strains by 2D analysis after experimental transmission

A lot of experimental transmission studies have been performed to define prion strains from small animals such as mice or hamster to highly evolved primates such as chimpanzees or macaques. Transmission studies in transgenic mice, carrying one or more human or bovine prion gene copy, are often a useful approach to investigate the relationship among different prion strains [22].

Nevertheless primates can be considered the host nearest to humans. In fact, several interesting similarities between human and cattle strains can be enhanced by molecular analysis after transmission experiments to primates.

sCJD MM-1 and sCJD MM-1 after experimental transmission to primate share identical patterns of PrP₂₇₋₃₀ and C-terminal fragments (CTFs) indicating that PrP^{Sc} fingerprints are conserved throughout transmission as reported in **Figure 14**. This finding confirms that primates are a good model to simulate transmission to humans of human prion strains.

In **Figure 15**, it can be noted that C-BSE shows the appearance of CTFs after first passage transmission, which maintains an identical pattern at second passage.

vCJD and vCJD passaged to primate share the same PrP^{TSE} fingerprints identical to those observed in BSE at first and second passage (**Figure 16**). This is a further confirmation of the correlation between BSE and vCJD.

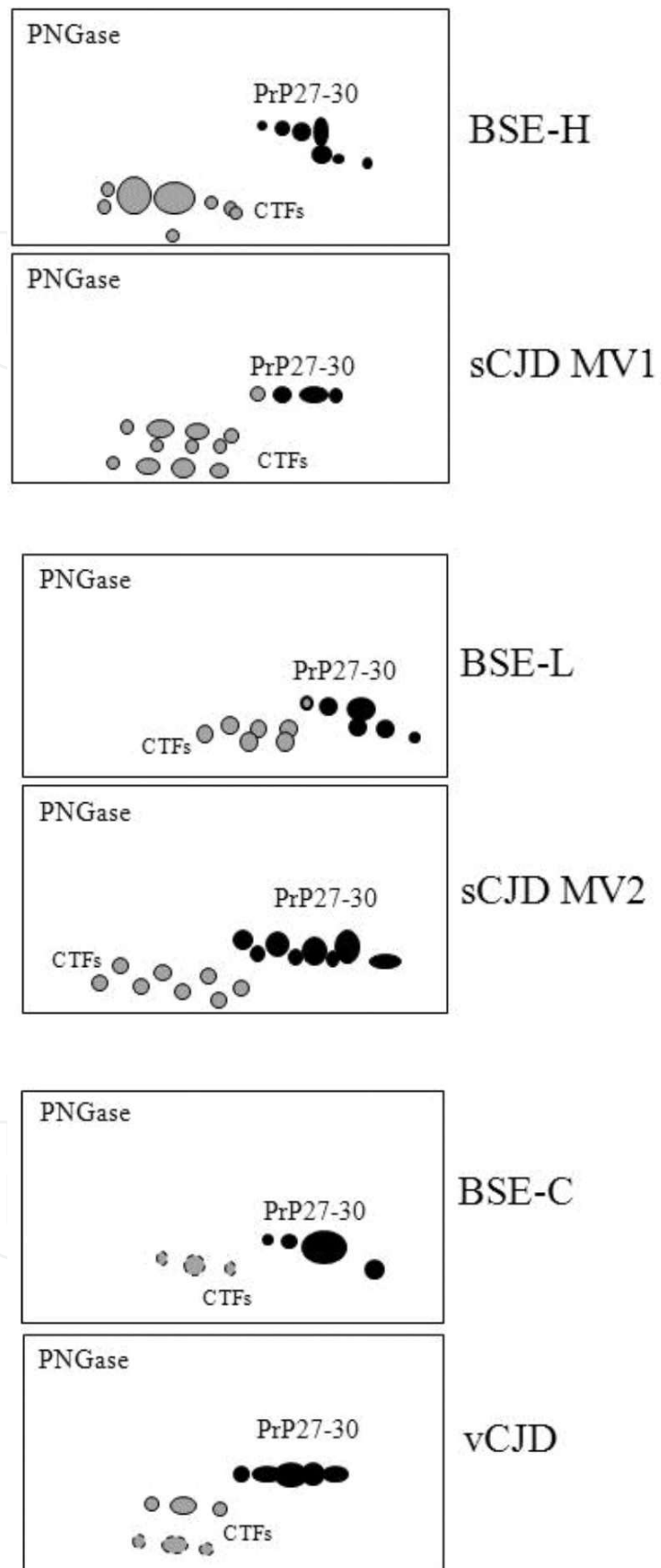


Figure 13. 2D western blot comparison between human and cattle TSE.

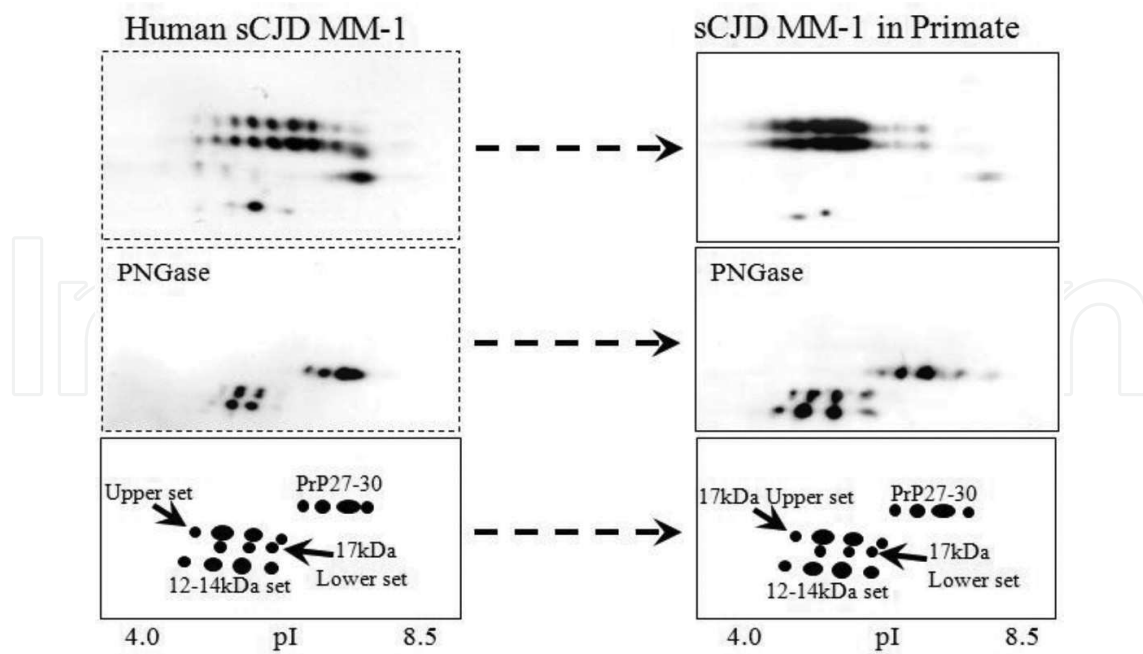


Figure 14. 2D western blot comparison between human MM-1 before and after transmission to primate.

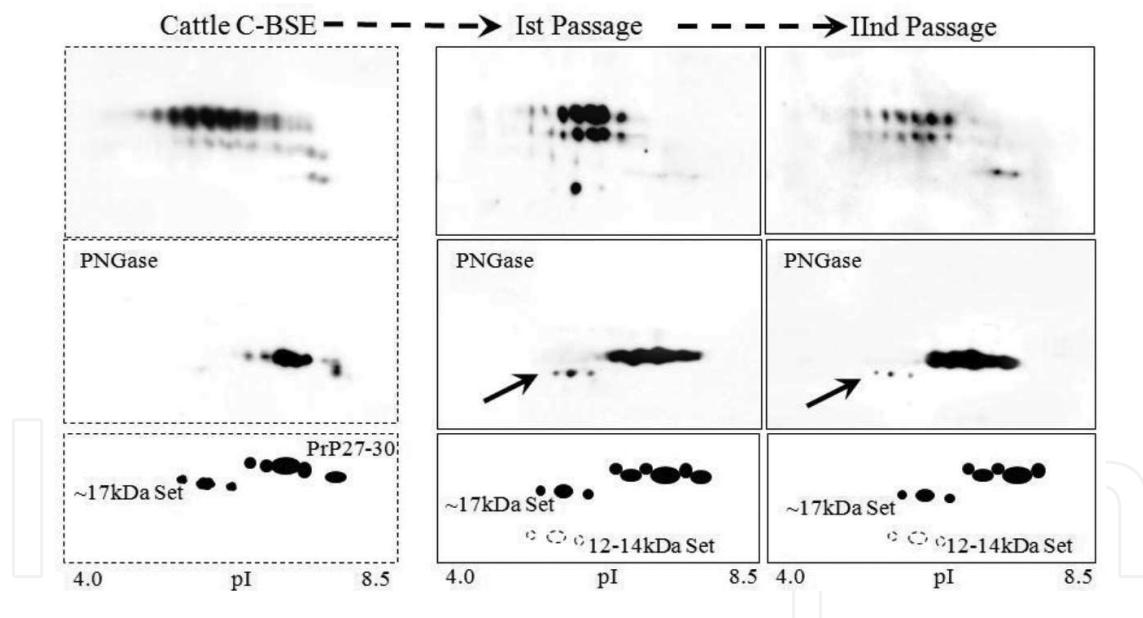


Figure 15. 2D western blot comparison between C-BSE before and after transmission at first and second passage to primate.

Figure 17 shows L-BSE PrP^{TSE} CTFs pattern in primate similar to that of L-BSE in cattle, characterized by a set of fragments migrating at 18 kDa; this set of spots are absent in BSE and vCJD passaged to primates. It's to be noted that L-BSE transmitted to primate is almost identical to human MV-2. These molecular signature similarities confirm molecular pattern previously observed for 1D immunoblot and suggests a possible molecular common origin of the two molecular strains. This correlation however needs to be deeply analyzed and confirmed.

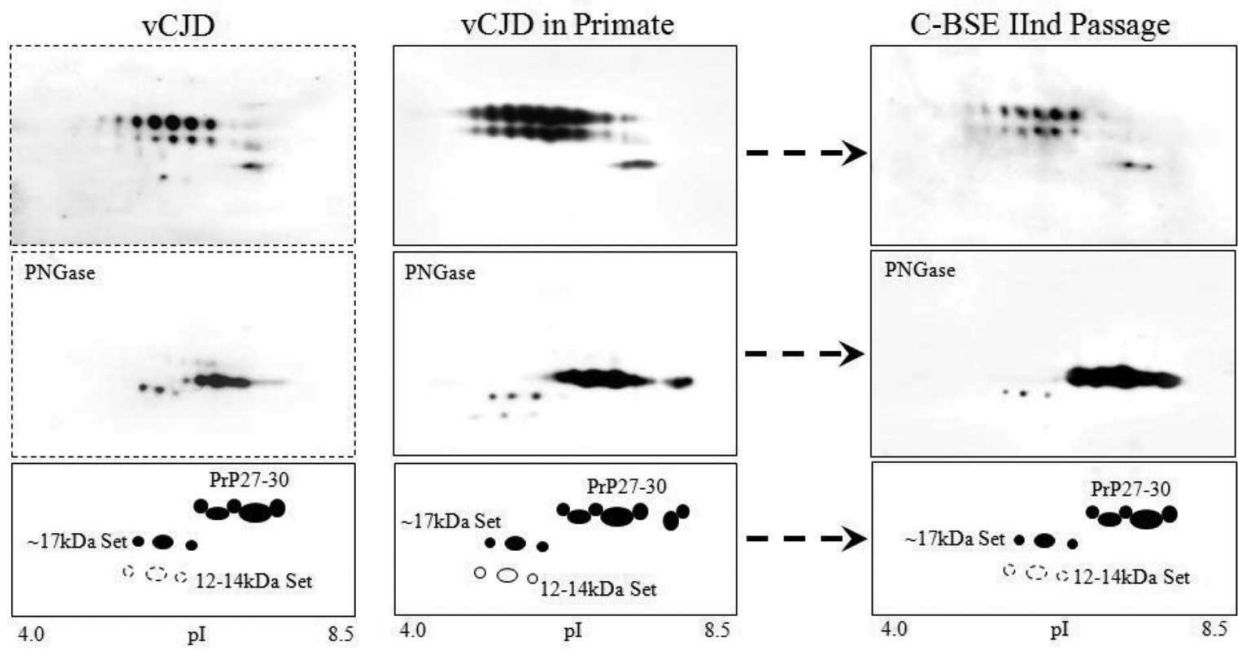


Figure 16. 2D western blot comparison between vCJD before and after transmission to primate and C-BSE after second passage to primate.

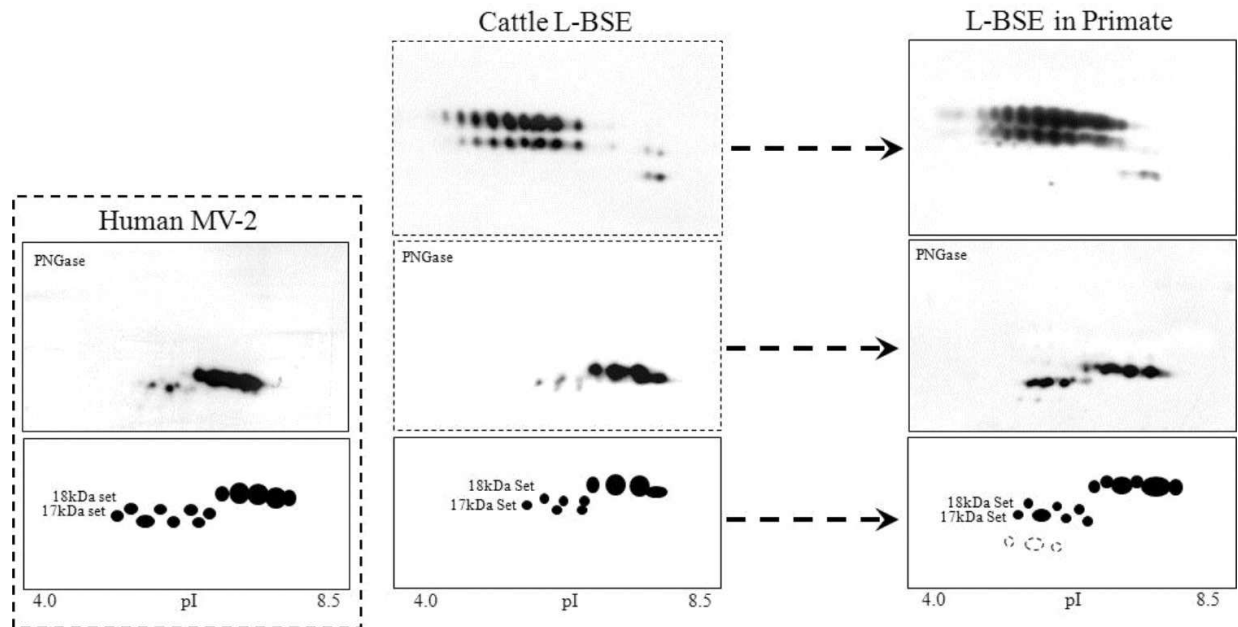


Figure 17. 2D western blot comparison between L-BSE before and after transmission to primate.

3. Conclusions

We have shown that molecular analysis of prions is a powerful approach to characterize prions.

By using several different biochemical approaches, it's possible to enhance molecular differences and similarities to define prion strains.

In particular, biochemical analysis is shown to be rapid and informative in:

- differentiation of PrP^{TSE} strains;
- correlation of molecular to clinicopathological phenotypes;
- large scale epidemiological studies and surveillance: finding and discriminating strains (sCJD, vCJD, atypical BSEs).

Author details

Michele Fiorini*, Matilde Bongianini and Gianluigi Zanusso

*Address all correspondence to: michele.fiorini@univr.it

Department Neurosciences, Biomedicine and Movement Sciences, University of Verona, Italy

References

- [1] Prusiner SB. Prions. *Proc Natl Acad Sci USA*. 1998;**95**(23):13363–83.
- [2] Basler K, Oesch B, Scott M, Westaway D, Wälchli M, Groth DF, McKinley MP, Prusiner SB, Weissmann C. Scrapie and cellular PrP isoforms are encoded by the same chromosomal gene. *Cell*. 1986;**46**(3):417–28.
- [3] Zanusso G, Fiorini M, Ferrari S, Meade-White K, Barbieri I, Brocchi E, Ghetti B, Monaco S. Gerstmann-Sträussler-Scheinker disease and “anchorless prion protein” mice share prion conformational properties diverging from sporadic Creutzfeldt-Jakob disease. *J Biol Chem*. 2014 Feb 21;**289**(8):4870–81. DOI: 10.1074/jbc.M113.531335
- [4] McKinley MP, Prusiner SB. Biology and structure of scrapie prions. *Int Rev Neurobiol*. 1986;**21**:1–57.
- [5] Bazan JF1, Fletterick RJ, McKinley MP, Prusiner SB. Predicted secondary structure and membrane topology of the scrapie prion protein. *Protein Eng*. 1987;**1**(2):125–35.
- [6] Safar J, Wille H, Itri V, Groth D, Serban H, Torchia M, Cohen FE, Prusiner SB. Eight prion strains have PrP^{Sc} molecules with different conformations. *Nat Med*. 1998;**4**(10):1157–65.
- [7] Bode L, Pocchiari M, Gelderblom H, Diring H. Characterization of antisera against scrapie-associated fibrils (SAF) from affected hamster and cross-reactivity with SAF from scrapie-affected mice and from patients with Creutzfeldt-Jakob disease. *J Gen Virol*. 1985;**66**(11):2471–8.
- [8] Hill AF, Joiner S, Wadsworth JD, Sidle KC, Bell JE, Budka H, Ironside JW, Collinge J. Molecular classification of sporadic Creutzfeldt-Jakob disease. *Brain*. 2003;**126**(6):1333–46.

- [9] Parchi P, Giese A, Capellari S, Brown P, Schulz-Schaeffer W, Windl O, Zerr I, Budka H, Kopp N, Piccardo P, Poser S, Rojiani A, Streichemberger N, Julien J, Vital C, Ghetti B, Gambetti P, Kretzschmar H. Classification of sporadic Creutzfeldt-Jakob disease based on molecular and phenotypic analysis of 300 subjects. *Ann Neurol*. 1999;**46**(2):224–33.
- [10] Zanusso G, Polo A, Farinazzo A, Nonno R, Cardone F, Di Bari M, Ferrari S, Principe S, Gelati M, Fasoli E, Fiorini M, Prelli F, Frangione B, Tridente G, Bentivoglio M, Giorgi A, Schininà ME, Maras B, Agrimi U, Rizzuto N, Pocchiari M, Monaco S. Novel prion protein conformation and glycoform in Creutzfeldt-Jakob disease. *Arch Neurol*. 2007;**64**(4):595–9.
- [11] Zou WQ, Puoti G, Xiao X, Yuan J, Qing L, Cali I, Shimoji M, Langeveld JP, Castellani R, Notari S, Crain B, Schmidt RE, Geschwind M, Dearmond SJ, Cairns NJ, Dickson D, Honig L, Torres JM, Mastrianni J, Capellari S, Giaccone G, Belay ED, Schonberger LB, Cohen M, Perry G, Kong Q, Parchi P, Tagliavini F, Gambetti P. Variably protease-sensitive prionopathy: A new sporadic disease of the prion protein. *Ann Neurol*. 2010;**68**(2):162–72. DOI: 10.1002/ana.22094.
- [12] Tagliavini F, Prelli F, Ghiso J, Bugiani O, Serban D, Prusiner SB, Farlow MR, Ghetti B, Frangione B. Amyloid protein of Gerstmann-Sträussler-Scheinker disease (Indiana kindred) is an 11 kd fragment of prion protein with an N-terminal glycine at codon 58. *EMBO J*. 1991;**10**(3):513–9.
- [13] Tagliavini F, Prelli F, Porro M, Rossi G, Giaccone G, Farlow MR, Dlouhy SR, Ghetti B, Bugiani O, Frangione B. Amyloid fibrils in Gerstmann-Sträussler-Scheinker disease (Indiana and Swedish kindreds) express only PrP peptides encoded by the mutant allele. *Cell*. 1994;**79**(4):695–703.
- [14] Piccardo P, Dlouhy SR, Lievens PM, Young K, Bird TD, Nochlin D, Dickson DW, Vinters HV, Zimmerman TR, Mackenzie IR, Kish SJ, Ang LC, De Carli C, Pocchiari M, Brown P, Gibbs CJ Jr, Gajdusek DC, Bugiani O, Ironside J, Tagliavini F, Ghetti B. Phenotypic variability of Gerstmann-Sträussler-Scheinker disease is associated with prion protein heterogeneity. *J Neuropathol Exp Neurol*. 1998;**57**(10):979–88.
- [15] Collinge J, Sidle KC, Meads J, Ironside J, Hill AF. Molecular analysis of prion strain variation and the aetiology of 'new variant' CJD. *Nature*. 1996;**383**(6602):685–90.
- [16] Shaked GM, Fridlander G, Meiner Z, Taraboulos A, Gabizon R. Protease-resistant and detergent-insoluble prion protein is not necessarily associated with prion infectivity. *J Biol Chem*. 1999;**274**(25):17981–6.
- [17] Peretz D, Scott MR, Groth D, Williamson RA, Burton DR, Cohen FE, Prusiner SB. Strain-specified relative conformational stability of the scrapie prion protein. *Protein Sci*. 2001;**10**(4):854–63.
- [18] Zanusso G, Farinazzo A, Prelli F, Fiorini M, Gelati M, Ferrari S, Righetti PG, Rizzuto N, Frangione B, Monaco S. Identification of distinct N-terminal truncated forms of prion protein in different Creutzfeldt-Jakob disease subtypes. *J Biol Chem*. 2004;**279**(37):389366–42.

- [19] Casalone C, Zanusso G, Acutis P, Ferrari S, Capucci L, Tagliavini F, Monaco S, Caramelli M. Identification of a second bovine amyloidotic spongiform encephalopathy: molecular similarities with sporadic Creutzfeldt-Jakob disease. *Proc Natl Acad Sci USA*. 2004;**101**(9):3065–70.
- [20] Polak MP, Zmudzinski JF, Jacobs JG, Langeveld JP. Atypical status of bovine spongiform encephalopathy in Poland: a molecular typing study. *Arch Virol*. 2008;**153**(1):69–79.
- [21] Lombardi G, Casalone C, D' Angelo A, Gelmetti D, Torcoli G, Barbieri I, Corona C, Fasoli E, Farinazzo A, Fiorini M, Gelati M, Iulini B, Tagliavini F, Ferrari S, Caramelli M, Monaco S, Capucci L, Zanusso G. Intraspecies transmission of BASE induces clinical dullness and amyotrophic changes. *PLoS Pathog*. 2008;**4**(5):e1000075. DOI: 10.1371/journal.ppat.1000075
- [22] Weissmann C, Enari M, Klöhn P-C, Rossi D, Flechsig E. Transmission of prions. *Proc Natl Acad Sci USA*. 2002;**99**(Suppl 4):16378–83.

